ELSEVIER

Bioelectrochemistry and Bioenergetics 48 (1999) 261–266

BIOELECTROCHEMISTRY AND BIOENERGETICS

Microelectronic sensors for measurement of electromagnetic fields of living cells and experimental results

František Jelínek [a,*], Jiří Pokorný [a], Jaroslav Šaroch [a], Viktor Trkal [a], Jiří Hašek [b], Bohuslav Palán [c]

[a] *Institute of Radio Engineering and Electronics, Academy of Sciences of Czech Republic, Chaberská 57, 182 51 Prague 8, Czech Republic*
[b] *Institute of Microbiology, Academy of Sciences of Czech Republic, Vídeňská 1083, 140 00 Prague 4, Czech Republic*
[c] *Faculty of Electrical Engineering, Czech Technical University in Prague, 160 00 Prague 6, Czech Republic*

Received 4 November 1998; received in revised form 8 December 1998; accepted 5 January 1999

Abstract

Microelectronic sensors are used for measurements of electromagnetic fields generated by synchronized cultures of yeast cells. Cold sensitive mutant *tub2-401* of *Saccharomyces cerevisiae* is used. The measured electromagnetic signals in the frequency range from 8 to 9 MHz are compared with evolution of the reassembled microtubules. The detected signals peak in the time interval 25–30 min and 45–60 min after the release of the cells from the restrictive to the permissive temperature. The first maximum corresponds to the stage when the mitotic spindle is formed and binds chromatids. The second maximum is measured when the processes of anaphase A and of anaphase B take place. © 1999 Elsevier Science S.A. All rights reserved.

Keywords: Microtubules electromagnetic activity; M phase; *Saccharomyces cerevisiae*

1. Introduction

Direct measurement of the electromagnetic field generated by living cells may deliver strong support for Fröhlich's theory of coherent oscillations in biological systems (the fundamentals of the Fröhlich theory may be found, e.g., in Refs. [1–4]). In our paper published in this journal in 1996 [5] we described an experimental laboratory system for detection of electromagnetic fields generated by living cells in the frequency range from 1 to 100 MHz. Now we shall describe some improvements of this experimental system and we shall give new results of our measurements.

Up to now only few direct measurements were performed and described in the literature [6]. The requirements to the measurement system are rather severe. The system has to be capable of detecting very weak nonhomogeneous electric fields in the vicinity of cellular membranes. The electric field is supposed to decrease very quickly with increasing distance from the membrane containing oscillation centres and reasonably great values may be expected within a distance of 0.1 μm. The electric power that can be expected may be of the order of 10^{-15} W or lower.

We measure the electromagnetic field generated by the synchronized yeast cells. The first measurements of the electromagnetic field generated by the yeast cells were published by H.A. Pohl [7] who used an indirect method based on dielectrophoretic effect. He observed attraction of small dielectric particles to cells. In the M phase of the cell cycle the yeast cell attracts the greatest number of particles, i.e., it emits the strongest field [8]. In the M phase the microtubules in cytoskeleton have a dominant role in the cell.

The microtubules form a highly dynamic structure. Generally, the microtubules are the main organizers of the cell. In the M phase they assemble in the mitotic spindle. Description of microtubules and their properties may be found, e.g., in [9]. Microtubules are polar structures; their subunits—tubulin heterodimers—are electric dipoles [10–13]. A large amount of energy is supplied to microtubules from hydrolysis of guanosine triphosphate to guanosine diphosphate [14–16]. The frequencies of vibration of tubulins in microtubules are assessed in the frequency range below 1 GHz [17,18]. The microtubules are polar and can

* Corresponding author. Tel.: +420-2-688-1804; fax: +420-2-688-0222; e-mail: jelinek@ure.cas.cz

0302-4598/99/$ - see front matter © 1999 Elsevier Science S.A. All rights reserved.
PII: S0302-4598(99)00017-3

generate a strong near zone electric field [18,19]. We assume that the cytoskeleton generates the electromagnetic field around cells also [18].

In yeast the microtubules emanate from the microtubule organizing center, called spindle pole body, that is embedded in the nuclear membrane. Therefore, two classes of microtubules should be distinguished: intranuclear (interpolar and kinetochore) and extranuclear (also called cytoplasmic). The distribution and length of these two types of microtubules change through the cell cycle. The function of the microtubule cytoskeleton appears to be limited to movement of the chromosomes and movement of the nucleus.

Fig. 1 shows the cell cycle of a yeast cell [20]. Part (a) of the figure shows a yeast cell with a bud. The cell enters the cycle. Two separate spindle pole bodies (SPB) are observed. The boundary between the G2 phase and the M phase is just after this stage (G2/M stage). The *tub2-401* mutant is arrested at this boundary as the microtubules cannot be polymerized at the restrictive temperature.

Part (b) of the figure shows the complete mitotic spindle. Two SPB's are positioned at the opposite sides of the nucleus (in yeast cells the nuclear membrane remains intact during mitosis), the intranuclear and extranuclear (cytoplasmic) microtubules are polymerized. The kinetochore microtubules bind chromatids (chromatids—two chromosomes bound with kinetochores).

Part (c) of the figure shows the anaphase stage. In the first part of the anaphase (anaphase A) the kinetochore microtubules shorten and the chromosomes are pulled toward the spindle pole body they face. During the anaphase B the interpolar microtubules elongate and the two spindle pole bodies move farther apart. The cytoplasmic microtubules direct the dividing nucleus into the bud.

Part (d) of the figure shows the cytokinesis stage of the M phase.

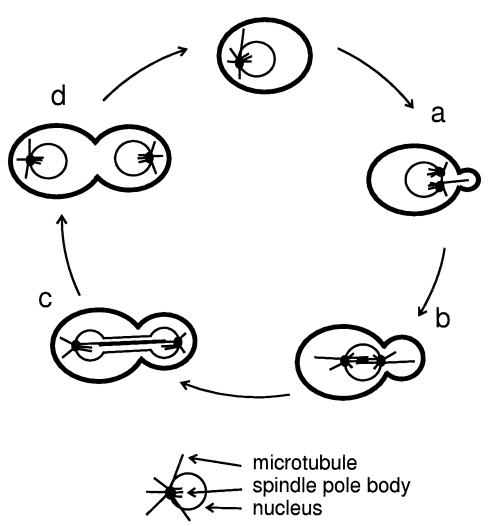


Fig. 1. *Saccharomyces cerevisiae* microtubule cytoskeleton in the mitotic cycle. After Ref. [20].

As the microtubule structure is polar and the energy supply in the M phase is great we may expect the greatest electric field generated by cells in this phase. Experimental findings of H.A. Pohl confirm this assumption.

2. Materials and methods

2.1. Yeast cell preparation

We measured the emission of synchronized yeast cells *Saccharomyces cerevisiae* with genetic mutation.

Cold sensitive mutant *tub2-401* (β-tubulin) [21] of *S. cerevisiae* was cultivated at the restrictive temperature (14°C) for 4 h. The cell cycle proceeds up to the end of the G2 phase and stops before entering the M phase. No microtubule structures are present. The cell cycle arrest point associated with the lack of microtubules is often used as a standard for mitotic arrest.

After the shift to the permissive temperature (≥ 25°C) the cells reassemble the microtubules and enter the M phase. Before measurements the cells were washed three times in deionized 0.06 M sucrose and resuspended in 0.06 M sucrose at 14°C.

2.2. Biological essay of the M phase

The cells were prepared as described by Hašek and Streiblová [21]. The fluorescence technique was used to visualize the microtubule structures.

Fluorescent micrographs were taken after the release of *tub2-401* cells from the restrictive to the permissive temperature. To obtain the microtubule fluorescence the following primary and secondary antibodies were used: The primary antibody was rabbit polyclonal antibody 206-1 against C-terminal domain of the yeast β-tubulin (Tub2p). This antibody was kindly provided by Prof. F. Solomon from MIT. The secondary antibody was goat antirabbit IgG conjugated with the CY3 fluorescent tag (Sigma).

2.3. Detection electrodes—sensors

Our experimental system for detection of living-cell oscillations was described and its block diagram was shown in the paper [5]. In the meantime we improved the sensitivity of the system which is now at the level of about 10^{-17} W in the frequency range from 1 to 10 MHz. Detection electrodes are the key part of the system. We have designed and prepared two types of sensors: metal strip on glass substrate and microelectronic configuration of electrodes on silicon substrate.

The preparation of the first type was done in a high vacuum 2.6×10^{-5} Pa. Pairs of metal strips 400 μm wide with a composition of 30 nm Ti/200 nm Au were evaporated on a glass substrate through a metal mask. The strips were broadened at the ends to form contacting pads. Then

an isolating layer of SiO_2 was evaporated on the surface of electrodes. At places where measured living cells should be inserted 8 μm wide gaps in this layer were formed by etching. Finally, to improve the electric interruption of the strip electrodes in the gap a spark discharge was applied. A miniature cuvette was formed on the glass plate. The sensor is schematically shown in Fig. 2.

The second type, microelectronic sensors, are developed in cooperation with the Institute of Radio Engineering and Electronics and the Innovation Centre of Microelectronics and Faculty of Electrical Engineering. The microelectronic chip is realized in CMOS technology. Seven pairs of metal strips are formed on a silicon substrate with dimensions 5 mm × 5 mm, covered by an isolating SiO_2 layer 3 μm thick. The widths of strips are about 10 μm and the gap between strips in a pair increases from pair to pair from 2 μm to larger widths in a sequence. The electrodes are covered by a CVD SiO_2 layer. Only above the gap between electrodes a square window is etched. This window is intended for inserting cells. The layout of the sensor chip is shown in Fig. 3a and a detail of the chip is shown in Fig. 3b. Dimensions of contact electrodes and windows are given in Table 1. A microscope photograph of one pair of strips digitally processed is shown in Fig. 4.

2.4. Measurements

The sensor chip together with the following amplifier are placed into a double-shielded box (electric and magnetic shielding).The first stage of the amplifier performs impedance matching and enables detection of the signal of the power of 10^{-17} W. The amplifier is connected to a spectrum analyzer [5]. Spectral analyser ANRITSU is used. The scanning time in the frequency range 8–9 MHz is 100 s, the resolution and the video bandwidth is 300 Hz.

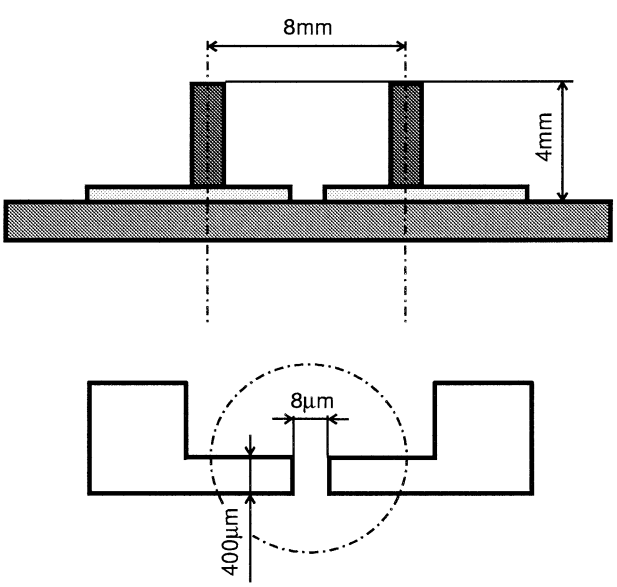


Fig. 2. Schematic illustration of a sensor with two golden strips evaporated on a glass substrate.

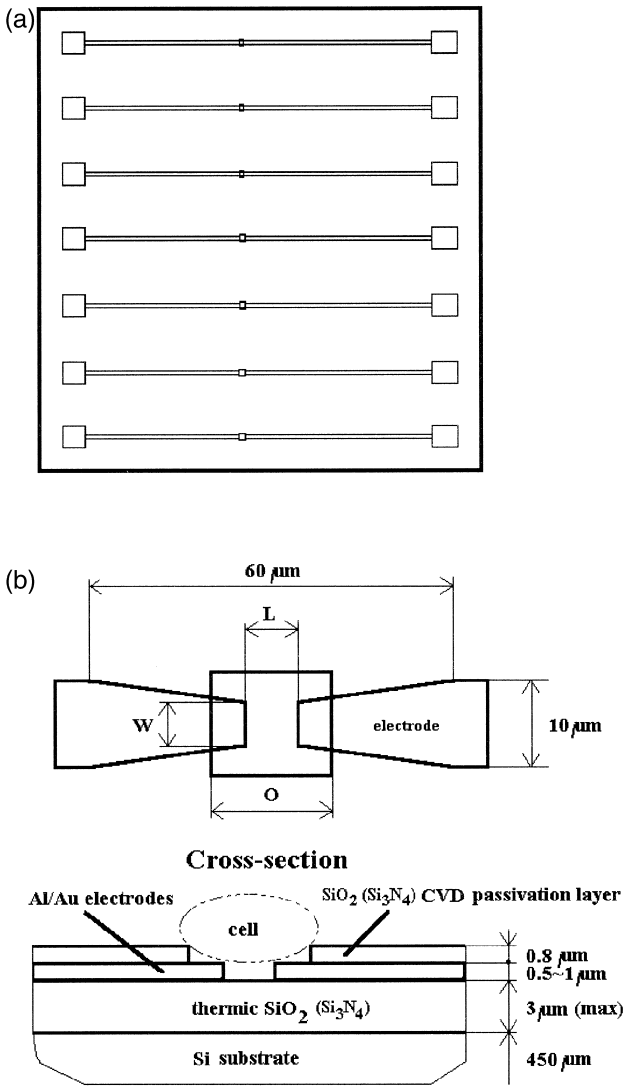


Fig. 3. A schematic illustration of the microelectronic sensor. The layout of metal strips on the chip (5 mm × 5 mm) (a) and detail of one electrode pair and the vertical cross-section of the layered structure (b).

Cell culture in deionized 0.06 M sucrose is heated in a water bath at 30°–34°C for 3 min and then given into a small cuvette around the contacts with the gap of the sensor or into a small window with contacts of the microelectronic sensor. The temperature during measurements is 25°–28°C. The beginning of heating in the water bath is

Table 1
Dimensions of contact electrodes

Window	L (μm)	W (μm)	O (μm)
1	2	2	7×7
2	3	3	8×8
3	4	3	9×9
4	5	3	10×10
5	6	3	11×11
6	7	3	12×12
7	10	3	15×15

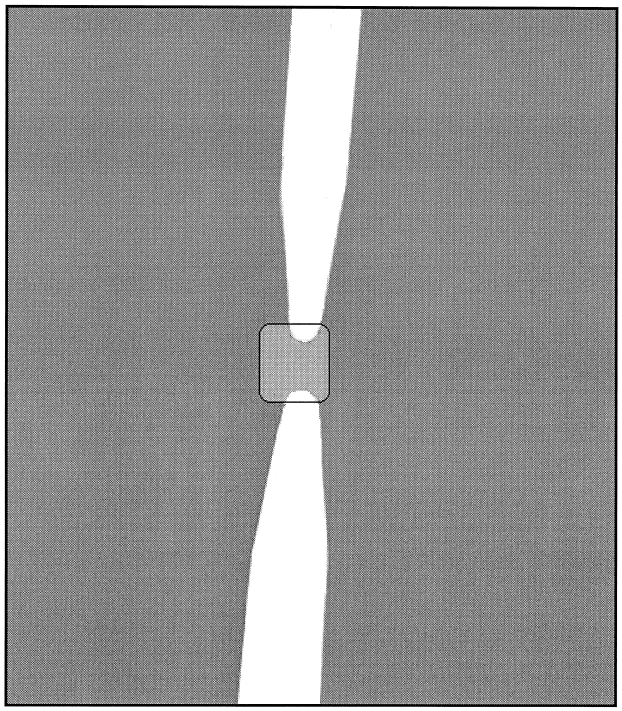


Fig. 4. Microscope image of a microelectronic sensor with two metal strips on a silicon substrate. The width of strips is about 10 μm and the gap between strips is about 6 μm.

the initial time ($t = 0$) for each experiment. We have to remark that the transition from the restrictive temperature to the permissive temperature is delayed with respect to the initial time.

Fig. 5 shows the result of one measurement of cells—the spectrum of a signal at the output of our experimental system with a microelectronic sensor at the input. The signal spectrum shown in Fig. 5 with a peak at the frequency 8.18 MHz exceeding markedly (of about 12–15 dB) a noise background was recorded 23 min after the initial time.

Control measurements are carried out with pure 0.06 M sucrose solution under the same conditions. We measured in the time interval 60 min after the initial time.

2.5. Evaluation of the results

The graphical records of the measured signal show large peaks greater then the noise (Fig. 5). The signal peaks greater than about 8 dB above the mean value of the noise were taken for evaluation. We summed the number of peaks in 5-min intervals for cell suspension (P_Y) and pure sucrose solution (P_C) and determined the difference $P_Y - P_C$ for one experiment.

3. Reassembly of microtubules

We observed microtubule structures in the *tub2-401* mutant released from restrictive to permissive temperature. Fluorescence micrographs represent distribution of β-tubulin stained with antibodies (Fig. 6).

Fig. 6a shows the state in the beginning, i.e., in the initial time ($t = 0$). The spherical nuclei with two spindle pole bodies are visible. The cells are at the boundary between the G2 phase and the M phase.

Fig. 6b shows the state 20 min from the beginning. The nuclei are elongated with complete mitotic spindle.

Fig. 6c shows the at time 40 min. The majority of the cells is in anaphase A. The mitotic spindles of these cells are elongated. Some cells in the population are in anaphase B (the spindles are very much elongated). As the anaphase A and anaphase B typically last about 1 min the cells enter in these stages in different moments.

Fig. 6d shows the state at time 60 min. The mitotic spindles of the majority of cells is very long (anaphase B), and some cells completed anaphase B.

4. Electromagnetic activity of yeast cells

We calculated the average values $P_Y - P_C$ from 14 experiments using a sensor with wide contacts (400 μm) on glass substrate. The result is shown in Fig. 7. The electromagnetic activity appears within the first 25 min after transition from the initial time when the temperature began to increase from the restrictive to the permissive one. In this period the spindle pole bodies are positioned to opposite sides of the nucleus, the intranuclear and extranuclear microtubules are polymerized, the mitotic spindle formed, and kinetochore microtubules bind chromatids. It has been often assumed that the short spindle stage represents the equivalent of metaphase in animal and plant cells, but there is no indication that yeast has true metaphase in terms of the morphology of the spindle.

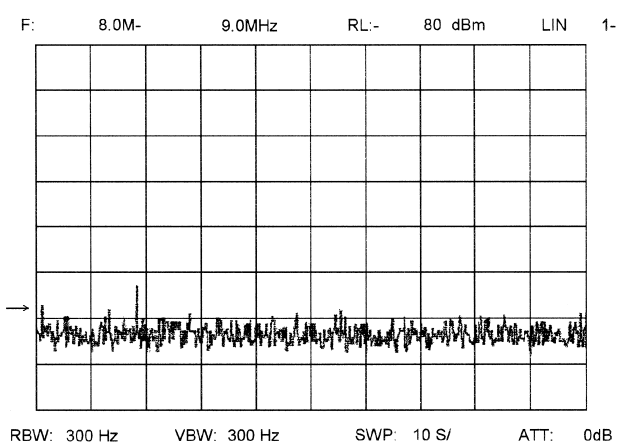


Fig. 5. Signal spectrum at the output of the experimental system with microelectronic sensor at its input. The square window of the microelectronic sensor was filled with the suspension containing yeast cells in the mitotic phase. The arrow on the left-hand side indicates the evaluation level (the signal peaks exceeding this level were taken for evaluation).

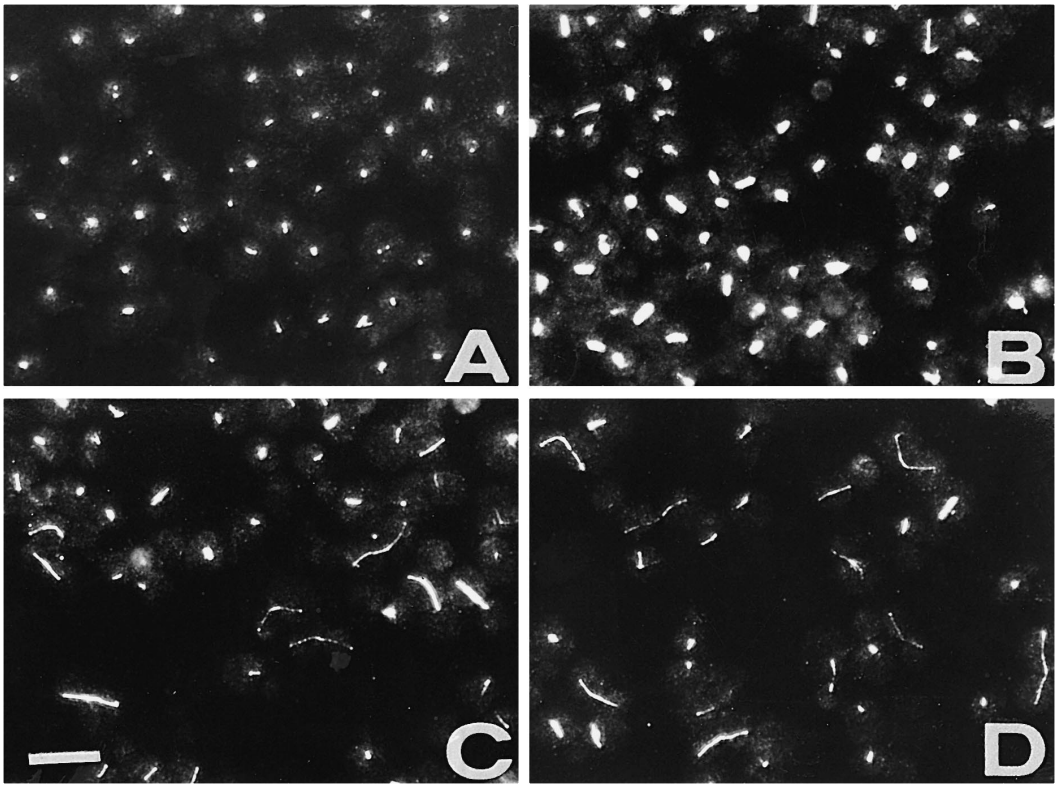


Fig. 6. Reassembly of microtubules in *tub2-401* mutant released from restrictive to permissive temperature. (a) $t = 0$, (b) $t = 20$ min, (c) $t = 40$ min, (d) $t = 60$ min. The horizontal bar in the lower left corner (c) indicates the distance, 10 μm.

The first maximum of the electromagnetic activity is in the time interval 25 to 30 min from the beginning. This seems to correspond to the beginning of the metaphase stage when the kinetochore microtubules bind the chromatids to the spindle pole bodies.

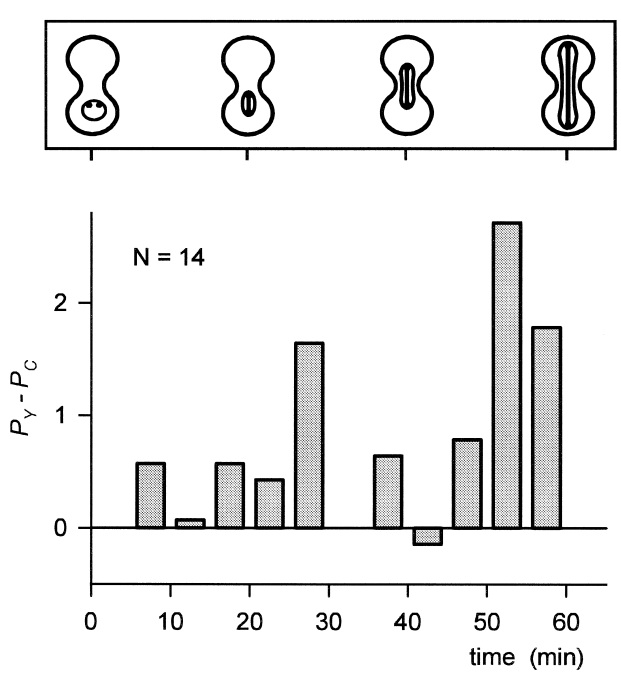


Fig. 7. Average values of the difference $P_Y - P_C$ calculated from 14 experiments in the time interval 0–60 min after increase of temperature. The schematic picture of reassembly of microtubules is shown in the upper part of the figure.

The electromagnetic activity increases again at 45 min from the beginning. In this time the anaphase stage starts abruptly. During the anaphase A the chromosomes are pulled towards the spindle pole bodies they face (the kinetochore microtubules shorten). This process in particular cells typically lasts shortly (about 1 min). After the anaphase A during the anaphase B the interpolar (pole to pole) microtubules elongate and the two spindle pole bodies move apart.

The second maximum of the electromagnetic activity appears in the time interval 50 to 60 min after the beginning. In this interval the majority of cells proceeds in the anaphase B processes.

5. Discussion

The sensor is one of the most important parts of the measurement systems. The contacts of the sensors with the glass substrate are 400 μm wide. The cell ‘diameter’ is about 8 μm or less. The signal generated by a cell is collected by a narrow patch of the wide contacts. The remaining part (which is the majority of the contacts) very likely deteriorates the signal by a parallel leakage. The

leakage of the signal decreases its amplitude. Additional noise might appear.

The substrate material is glass which has undefined surface properties. The ionic conductivity at the surface can deteriorate the performance of the sensor and generate noise signals. The microelectronic sensors with Au contacts 10-μm wide have strongly diminished parallel leakage if the window exposing the tips of the contacts is not too large. The passivated surface of the chip by SiO_2 seems to be more convenient than the surface of glass. Nevertheless, the isolating layer from SiO_2 above the contacts may be degraded by water.

The volume of the cuvette with the measured suspension is small. The cells form a continuous layer at the bottom. The conditions for cell development are not quite normal.

The measured peaks manifest electromagnetic activity of yeast cells. The present state of measurements does not enable us to determine the level of coherence of the signal. Further improvements of the method are necessary in this respect or a new method has to be used (e.g., a method based on the Mössbauer effect [22]).

The power of the cell signal is of the order of 10^{-15} W or lower and the noise fluctuations may be of the same order of magnitude. The noise has several components that originate in the interface between the suspension and the substrate with contacts, in the 'wires' connecting the sensor with the amplifier, and in the input stage of the amplifier. Motion of cells in the gap between the contacts may also contribute to the noise (in particular, in the initial time). The contribution to noise from the 'wire' connections to the amplifier can be reduced using hybrid sensors where the low-noise amplifier is integrated with the sensor. The remaining noise could be eliminated by statistical methods of evaluation.

6. Conclusions

We may conclude that the electromagnetic signals are generated in the M phase of the cell cycle of the measured synchronized yeast cells. We compare the electromagnetic activity with reassembly of microtubules. We connect these signals with the microtubule activity as the microtubules are the main organizers of the M phase; they are the 'working' structures with energy supply. These findings are in agreement with the indirect (microdielectrophoretical) measurements of H.A. Pohl [7,8].

Acknowledgements

The work has been supported by the Grant Agency of the Czech Republic under contract No. 102/97/0867 and under the Action COST 244bis.

References

[1] H. Fröhlich, in: M. Marois (Ed.), Quantum Mechanical Concepts in Biology, Theoretical Physics and Biology, North-Holland, Amsterdam, 1969, pp. 13–22.
[2] H. Fröhlich, Bose condensation of strongly excited longitudinal electric modes, Phys. Lett. A 26 (1968) 402–403.
[3] H. Fröhlich, Long-range coherence and energy storage in biological systems, Int. J. Quantum Chem. II (1968) 641–649.
[4] H. Fröhlich, The biological effects of microwaves and related questions, Adv. Electron. Electron Phys. 53 (1980) 85–152.
[5] F. Jelínek, J. Šaroch, V. Trkal, J. Pokorný, Measurement system for experimental verification of Fröhlich electromagnetic field, Bioelectrochem. Bioenerg. 41 (1996) 35–38.
[6] R. Hözel, I. Lamprecht, Electromagnetic field around biological cells, Neural Network World 4 (1994) 327–337.
[7] H.A. Pohl, Oscillating fields about growing cells, Int. J. Quantum Chem.: Quantum Biol. Symp. 7 (1980) 411–431.
[8] H.A. Pohl, T. Braden, S. Robinson, J. Piclardi, D.G. Pohl, Life cycle alterations of the mico-dielectrophoretic effects of cells, J. Biol. Phys. 9 (1981) 133–154.
[9] B. Alberts, D. Bray, J. Lewis, M. Raff, K. Roberts, J.D. Watson, Molecular Biology of the Cell, Garland Publishing, New York, 1994.
[10] M.V. Satarić, J.A. Tuszyński, R.B. Žakula, Kinklike excitations as an energy-transfer mechanism in microtubules, Phys. Rev. E 48 (1993) 589–597.
[11] M.V. Satarić, J.A. Tuszyński, S. Hameroff, R.B. Žakula, Microtubules and their role in neuromolecular computing, Neural Network World 4 (1994) 281–294.
[12] J.A. Tuszyński, S. Hameroff, M.V. Satarić, B. Trpisová, M.L.A. Nip, Ferroelectric behavior in microtubule dipole lattices: implications for information processing, signaling and assembly/disassembly, J. theor. Biol. 174 (1995) 371–380.
[13] J.A. Tuszyński, B. Trpisová, D. Sept, From erratic to coherent behaviour in the assembly of microtubules, Neural Network World 5 (1995) 675–688.
[14] M. Caplow, R.L. Ruhlen, J. Shanks, The free energy for hydrolysis of a microtubule-bound nucleotide triphosphate is near zero: all of the free energy for hydrolysis is stored in the microtubule lattice, J. Cell Biol. 127 (1994) 779–788.
[15] M. Caplow, J. Shanks, Induction of microtubule catastrophe by formation of tubulin-GDP and apotubulin subunits at microtubule ends, Biochemistry 34 (1995) 15732–15741.
[16] M. Caplow, J. Shanks, Evidence that a single monolayer tubulin-GTP cap is both necessary and sufficient to stabilize microtubules, Mol. Biol. Cell 7 (1996) 663–675.
[17] J. Pokorný, F. Jelínek, V. Trkal, I. Lamprecht, R. Hölzel, Vibrations in microtubules, J. Biol. Phys. 23 (1997) 171–179.
[18] J. Pokorný, T.-M. Wu, Biophysical Aspects of Coherence and Biological Order, Academia, Prague, Springer, Berlin, 1998.
[19] J. Pokorný, F. Jelínek, V. Trkal, Electric field around microtubules, Bioelectrochem. Bioenerg. 45 (1998) 239–245.
[20] T.C. Huffaker, J.H. Thomas, D. Botstein, Diverse effects of β-tubulin on microtubule formation and function, J. Cell Biol. 106 (1988) 1997–2010.
[21] J. Hašek, E. Streiblová, in: I.H. Evans (Ed.), Fluorescence Microscopy Methods, Methods in Molecular Biology, Vol. 53, Humana Press, Totova, NJ, 1996, pp. 391–405.
[22] M.V. Satarić, S. Zeković, J.A. Tuszynski, J. Pokorný, Mössbauer effect as a possible tool in detecting nonlinear excitations in microtubules, Phys. Rev. E 58 (1998) in print.